Climatic Change (2022) 174:12
https://doi.org/10.1007/s10584-022-03359-2

Quantification of meteorological drought risks between 1.5 °C and 4 °C of global warming in six countries

Jeff Price[1] · Rachel Warren[1] · Nicole Forstenhäusler[1] · Craig Wallace[2] · Rhosanna Jenkins[1] · Timothy J. Osborn[2] · D. P. Van Vuuren[3]

Received: 28 August 2020 / Accepted: 24 April 2022 / Published online: 28 September 2022
© The Author(s) 2022

Abstract

We quantify the projected impacts of alternative levels of global warming upon the probability and length of severe drought in six countries (China, Brazil, Egypt, Ethiopia, Ghana and India). This includes an examination of different land cover classes, and a calculation of the proportion of population in 2100 (SSP2) at exposed to severe drought lasting longer than one year. Current pledges for climate change mitigation, which are projected to still result in global warming levels of 3 °C or more, would impact all of the countries in this study. For example, with 3 °C warming, more than 50% of the agricultural area in each country is projected to be exposed to severe droughts of longer than one year in a 30-year period. Using standard population projections, it is estimated that 80%-100% of the population in Brazil, China, Egypt, Ethiopia and Ghana (and nearly 50% of the population of India) are projected to be exposed to a severe drought lasting one year or longer in a 30-year period. In contrast, we find that meeting the long-term temperature goal of the Paris Agreement, that is limiting warming to 1.5 °C above pre-industrial levels, is projected to greatly benefit all of the countries in this study, greatly reducing exposure to severe drought for large percentages of the population and in all major land cover classes, with Egypt potentially benefiting the most.

Keywords Meteorological drought · SPEI · Climate change and warming · CMIP5

This article is part of the topical collection "Accrual of Climate Change Risk in Six Vulnerable Countries", edited by Daniela Jacob and Tania Guillén Bolaños'

✉ Rachel Warren
R.Warren@uea.ac.uk

Jeff Price
jeff.price@uea.ac.uk

[1] Tyndall Centre for Climate Change Research, School of Environmental Sciences, University of East Anglia, Norwich NR4 7TJ, UK

[2] Climatic Research Unit, School of Environmental Sciences, University of East Anglia, Norwich NR4 7TJ, UK

[3] PBL Netherlands Environmental Assessment Agency, The Hague, the Netherlands

1 Introduction

In this paper the level of risk that climate change poses to six countries (Brazil, China, Egypt, Ethiopia, Ghana and India) in terms of changes in meteorological drought is projected, using a variety of metrics quantifying the duration, frequency and severity of the projected drought for global warming levels of between 1.5 and 4 °C. A spatially explicit analysis is conducted at a scale of 0.5° latitude by 0.5° longitude (approx. 50 km by 50 km) after which the drought metrics are spatially averaged over each country as a whole. Finally, the exposure of agricultural land, natural land, permanent snow and ice (where relevant), and total numbers of people to the increased drought, as compared with an observational time period (1961–1990), is explored, using a standard projection of population (Shared Socioeconomic Pathway 2 (Jones and O'Neill 2016) to assess the human population exposure).

Drought can have major impacts on biodiversity, agricultural yields, water storage (including snow and ice) and flows, people and economies. For example, droughts in Europe have had an estimated annual economic impact of €5.3 billion since 1991 (in Feyen and Dankers 2009). There are many different metrics used for drought and the choice of metric depends on the questions asked and underlying data availability. An important distinction is between meteorological drought, which is dependent only upon in situ climatology and land use, and hydrological drought, which is also affected by runoff from upstream locations. Runoff and water scarcity are assessed in the sister paper in this Special Issue (He et al 2022), while this paper is restricted to the assessment of meteorological drought. The projected drought reported here is strictly related to in situ conditions and does not capture the indirect effects of drought occurring in other parts of the country, which might affect runoff, crop yields and local supply chains. The sister paper in this Special Issue (Wang et al 2021) addresses indirect effects of climate change induced changes in crop yields and thus reflects one potential mechanism for effects at larger scales.

While there are similarities (and, often, strong correlations) in the different metrics of meteorological drought (hereafter referred to as 'drought'), there can be significant differences as well, especially when projecting drought conditions under global warming conditions. For example, some drought metrics (e.g. Standardized Precipitation Index, SPI) are based solely on precipitation (P), some incorporate a measure of evaporative demand (dependent especially on temperature; e.g. Standardized Precipitation-Evapotranspiration Index, SPEI), and some take into account soil moisture (e.g. Palmer Drought Severity Index, PDSI). As SPI only utilizes precipitation, any area with increasing precipitation would show reduced levels of drought, even though temperature, and thus evaporation, also increases. Thus, SPI is not a very effective measure of drought under global warming. Similarly, the use of consecutive dry days (CDD) can give misleading results, as it does not take into account any increase in temperature-driven evaporation and long droughts. We therefore chose to use SPEI (Vicente-Serrano et al. 2010) to quantify long-term drought conditions in this study for these reasons.

Drought can occur over different time scales, ranging from a single month to years. Here we used SPEI over a 12-month timescale. That is, a drought of magnitude x (in this study, -1.5 (approximating 1.5 standard deviations, or worse)) based on the moisture deficit (P-PET, where P is the precipitation and PET the potential evapotranspiration) averaged over 12 months. This level of drought has been found to have impacts on both agriculture and groundwater supplies versus using drought lengths of shorter periods (Zhao et al. 2017). Using SPEI-12 helps avoid potentially misleading seasonally dependent results,

particularly in areas with clear wet and dry seasons. SPEI-12 is calculated as a moving average, so an SPEI-12 drought in a given month means that the average conditions in the current plus previous 11 months *average* to indicate drought conditions of this magnitude. While not every month may have been in drought (indeed, some could have excess moisture), the overall average equates to drought. Thus, when consecutive months of SPEI-12 drought are assessed, the overall length of drought is longer than the number of months indicated, as they are the consecutive months from the time the SPEI-12 drought has begun. Thus, 12 consecutive months of an SPEI-12 severe drought equates to a dry spell that might span 1–2 years when taking into account the development of the drought.

This study examined projected drought risk in China, Brazil, Egypt, Ethiopia, Ghana and India. These six countries provide a range of contrasting sizes and different levels of development on three continents spanning tropical and temperate biomes, and forest, grassland and desert habitats. There are many studies examining observed droughts in these countries using a range of drought indices. Pathak and Dodamani (2019) compared multiple meteorological drought indices for one river basin in India and found SPEI identified the highest number of drought events. SPI has also been widely used, including studies in Ghana (Volta River Basin, Kasei et al., 2010); India (Naresh Kumar et al. 2011); Eastern Nile Basin (Elkollaly et al. 2018); and China (Du et al. 2013). A crop drought vulnerability index developed for Ghana found the north of the country to be the most vulnerable, which is also the more arid region (Antwi-Agyei et al. 2012). An index quantifying the impacts of drought intensity on grain production in China from 1990–2011 showed that 25–30 million ha of cropping land were at risk of drought each year (Qin et al. 2014).

Table 1 summarises earlier work on drought projection in four of the countries studied. Some of the earlier work uses drought indices such as CDD or SPI that can produce misleading results. For example, use of SPI results in projections of reduced drought frequency across India as this indicator does not account for increases in evaporative demand (linked to rising temperature) in tandem with precipitation increases. We were unable to identify studies projecting future drought risk at the country level for Ethiopia or Egypt.

Thus, this paper builds and expands on previous work by: a) doing consistent analyses on six countries, including two previously under-studied, using SPEI, a more appropriate drought metric than the SPI or CDD metrics used in some of the earlier studies; b) looking at a consistent range of policy-relevant levels of global warming; c) examining the differential drought impacts in agricultural, natural, urban areas and areas with permanent snow and ice; d) examining percentages of people potentially at risk of being exposed to a severe drought averaging longer than a year; and e) examining the percent land area in different land cover classes exposed to a severe drought averaging longer than a year.

2 Data and methods

2.1 Climate data

Meteorological input data for the future were derived for eight global warming scenarios in which global average temperatures rise by < 1.5, 1.5, < 2, 2, 2.5, 3, 3.5 and 4 °C above pre-industrial levels. The two scenarios, < 1.5 °C and < 2 °C follow emissions pathways determined by the IMAGE model (Stehfest et al. 2014) to give a 66% chance of staying below 1.5 °C and 2 °C and then the median warming for each pathway is selected (which give global temperature rises of 1.43 °C and 1.76 °C, respectively). All remaining

Table 1 Previous studies of projected drought under climate change in Brazil, China, Ghana and India (for China, the most pertinent recent literature has been selected for highlight here)

Country	Drought indicator and climate scenarios	Key findings	Source
Brazil, NE	Annual consecutive dry days (CDD) 24 CMIP5 GCMs with the 4 standard RCPs for 2071–2100		Marengo et al. 2017
Southern half of S America	SPI 15 CMIP5 models under RCP4.5 and RCP8.5 for 2011–2040, relative to 1979–2008	10–20% increase in drought frequency, 5–15% increase in drought severity, but reduction in drought duration of 10 –30%	Penalba and Rivera (2015)
China	Palmer Drought Severity Index (PDSI) 35 CMIP5 GCMs RCP4.5 and RCP8.5 for 2020s, 2050s and 2080s	More extreme climate, in terms of both droughts and wet years. Droughts currently classified as extreme become the norm by the end of the century for RCP8.5. Drought more widespread, spreading across South-west China	Wang and Chen (2014), Wang et al. (2014)
China	Meteorological, agricultural and hydrological droughts 5 GCMs RCP8.5 for 2020–2049 relative to 1971–2000	Droughts more severe, prolonged, and frequent except in parts of northeast and north	Leng et al 2015
Ghana, Volta River Basin	SPI and SPEI 8 GCMs downscaled using the CORDEX-Africa regional climate model RCP4.5 and RCP8.5 for 2046–2065 and 2081–2100	Increased drought likelihood and drought area extent (more pronounced for SPEI than SPI). For SPEI, drought area extent increased from around 13% under baseline conditions to 24% in 2046–2065 and to 31% in 2081–2100 under RCP4.5; and to 29% and 34% in these periods under RCP8.5	Oguntunde et al. 2017
India	SPI, SPEI and Standardized Effective Precipitation Evapo-Transpiration Index (SP*ETI) 7 RCMs RCP4.5 and RCP8.5 for 2021–2050 and 2070–2100	Increasing drought across India, when SPEI used as the indicator. A shift in location of the greatest drought hazard from central India towards the southeast	Gupta and Jain (2018), Aadhar and Mishra (2018).

scenarios assume warming of exactly their respective temperature. Because no GCM has been run for this range of specific warming levels, we scaled the GCM-simulated patterns of climate change to match these specific warming levels using the ClimGen pattern-scaling technique (Osborn et al. 2016). By doing so, we assume a linear relationship between changes of a climate variable within a single grid cell and the change in global-mean surface temperature. To capture uncertainty in climate projections, we used scaling factors diagnosed from a total of 23 CMIP5 GCMs, a common strategy (see James et al. 2017; Tebaldi and Arblaster 2014; and Osborn et al. 2018 for application, strengths and limitations).

This also means that in projecting drought metrics at different levels of global warming, in each of the CMIP5 GCMs, a different time slice corresponds to the particular level of global warming such as 2 °C. This means that our exploration of regional climate projection quantifies uncertainties in the regional pattern of warming corresponding to, for example, 2 °C global warming, and not the uncertainty in the regional pattern of global warming in say a particular time period in the future. Hence, these projections are essentially independent of the decade in which they may occur.

For analysis of drought, future time series of meteorological variables (precipitation, mean, minimum and maximum temperature, cloud cover and vapour pressure) are needed. We generate 30-year monthly time series of these variables by combining observed variability from the 30-year reference period (1961–1990) with the pattern-scaled changes in mean climate between reference and future global warming levels (< 1.5 to 4 °C). The observed climate came from CRU TS 3.00 (Harris et al. 2014). Using observed variability rather than model-simulated variability avoids problems where model variability is unrealistic but by default prescribes the same variability for the future climate as for the observed climate. The latter limitation is overcome for precipitation (the variable for which changes in variability are the most important when considering drought) by modifying the default approach to also perturb the observed monthly precipitation variability according to the changes in precipitation variability simulated by the respective GCM. Thus, GCM projected changes in future precipitation variance and distribution skewness are included in the monthly series. Osborn et al. (2016; their figure 3) showed that this approach can emulate GCM projections of the frequency of dry months much better than the default approach in regions where a GCM projects a significant change in precipitation variability.

PET was calculated using a version of the Penman–Monteith formulation based on minimum, maximum and mean surface temperature, vapour pressure, cloud cover and the CRU CL 2.0 wind speed climatology (Harris et al. 2014). The climate data and derived drought metrics were all calculated at a spatial resolution of 0.5° latitude and longitude; hence, the grid cells used in our spatial analysis are approximately 50 × 50 km in size in most countries.

2.2 Drought metric

For this calculation, we used monthly P and PET from the data set described above. Following Vicente-Serrano et al. (2010) we first derived the differences between monthly P and PET (P-PET), converted them into 12-month running means (D) and fitted a log-logistic distribution to D in our observed calibration period (1961–1990). The resulting probability distribution function of the D series was used to estimate SPEI-12 for both observed and projected time-periods. Since the pattern scaling method projects the future

climate independently of time, the projections are valid for any future time period with the corresponding change in global temperature. However, once combined with a projected population for 2100 (SSP2), they are assigned to refer to a 30-year time slice centred on 2100.

Several metrics were derived from the estimated SPEI to provide a more detailed picture of drought conditions based on different SPEI thresholds. First, we determined the probabilities of droughts of a specific category occurring in each grid cell in each month of the 30-year time slice, by dividing the total number of months under drought conditions by the overall number of months (349, because 11 months are lost when forming a 12-month running mean). The results presented here are for SPEI-12 < = -1.5 which is the classification of severe (or worse) droughts. The SPEI-12 threshold of -1.5, or severe drought, is commonly used in drought impact studies and was supported by an informal discussion with a small group of stakeholders. The metric includes all values less than -1.5 (e.g. extreme drought), but used -1.5 as the starting point. It is also an appropriate threshold for the 30-year calibration period that we use: a value below -1.5 standard deviations will occur 6.7% of the time, i.e. typically, the 24 months with the most negative SPEI-12 values during the calibration period define what is at least a severe drought. A more extreme threshold (e.g. -2, -2.5, etc.) would be less well defined because such strongly negative values occur less frequently during the calibration period. Second, we looked at the total number of months in a drought category per year, the maximum number of consecutive months in a category per year and at the maximum number of consecutive months in a category per 30-year period. As noted above, there are a total of 349 monthly SPEI-12 values in each period. By calculating these three additional measures, we were able to not only quantify changes in frequency but changes in duration of drought events as well.

As described in the SM, drought metrics were calculated from all 23 sets of projections (each set arising from the climate change patterns obtained from a different GCM, and thus sampling the sensitivity of our results to choice of GCM). Here, we present the median of these 23 values.

The drought probability and drought length were analysed at an overall country level, as well as within different land cover classes within each country. The land cover classification comes from the European Space Agency Climate Change Initiative Land Cover Database (ESA CCI; 300 m resolution) for the year 2015 to maintain consistency with other parts of the project (e.g. Price et al. this volume). Resampling (ArcGIS Pro 2.4.1, Procedure RESAMPLE, nearest neighbour) was used to resample the original 0.5° drought data to match the 300 m resolution of the land cover data. These resampled rasters were then used to examine the potential impacts of drought on land identified as being > 50% agriculture, > 50% natural, urban areas (meaning areas with settlements of approximately 1 km^2 or larger, urban used to correspond to definition used in the land cover classification used), or permanent snow and ice. Drought metrics for each individual land cover classification can be found in the Supplementary Material, Tables SM1-12. Finally, the proportion of population in each country exposed to a -1.5 SPEI-12 drought was calculated using both constant population (2000) and the projected population for 2100 according to Shared Socioeconomic Pathway 2 (Jones and O'Neill 2016). Once combined with population estimates, the projections are then pinned to the year 2100. However, the full range of levels of global warming explored is consistent with SSP2 in 2100.

3 Results

For each country as a whole, the overall spatially averaged probability that any given month of the year is in the 'severe drought' category based on SPEI-12 is shown in Table 2. Drought probability is projected to increase in all countries relative to the observational period (1961–1990, Sect. 2.1). In the 1.5 °C warming scenario, the drought probability is projected to triple in Brazil and China, nearly double in Ethiopia and Ghana, increase slightly in India, and substantially increase in Egypt. Like most standardised metrics, SPEI can show apparently large changes in areas with already low precipitation and low interannual precipitation variability, as even small changes in precipitation may appear large relative to the standard deviation during the calibration period. Nevertheless, the increased probability of drought in, e.g. Egypt, is an indication both of the increase in evaporation and the increase in temperature. Under these conditions, drought may become more probable even where precipitation increases if the increase in PET is larger, while even minor decreases in precipitation could show as large increases in drought risk when combined with higher PET and when standardised against low present-day variability. This is especially important, as can be seen in later figures, in areas dependent on rainfed agriculture, settlements away from rivers, and many natural areas.

In a 2 °C warming scenario, the probability of drought is projected to quadruple in Brazil and China; double in Ethiopia and Ghana; reach greater than 90% probability in Egypt; and nearly double in India (Fig. 1). In a 3 °C warming scenario, the probability of drought projected to be in Brazil and China is 30%-40%; 20%-23% in Ethiopia and Ghana; 14% in India but nearly 100% in Egypt. Finally, in a 4 °C warming scenario, the probability of drought projected in Brazil and China is nearly 50%; 27%-30% in Ethiopia and Ghana; nearly 20% in India and 100% in Egypt. In most countries, the projected increase in drought probability increases approximately linearly with increasing temperature with the exception of Egypt, where even slight amounts of global warming potentially lead to large increases in drought probability (Fig. 1). There seems to be a slight jump in probability increase between the 2 °C and 2.5 °C warming scenarios in the other countries.

Table 2 The probability (%) that any given month will be classified as having a severe (or worse) drought (SPEI-12 < -1.5) at an individual grid cell, then averaged over all grid cells in each of the six countries examined in this study. Median of 23 GCM patterns

Country	Baseline	< 1.5	1.5 °C	< 2	2.0 °C	2.5 °C	3.0 °C	3.5 °C	4.0 °C
Brazil	6	19	21	24	28	34	40	44	48
China	6	17	19	21	25	31	36	41	45
Egypt	6	70	77	85	91	97	99	99	100
Ethiopia	6	10	11	12	14	17	20	24	27
Ghana	7	11	12	14	16	20	23	27	30
India	6	8	9	9	10	12	14	16	19

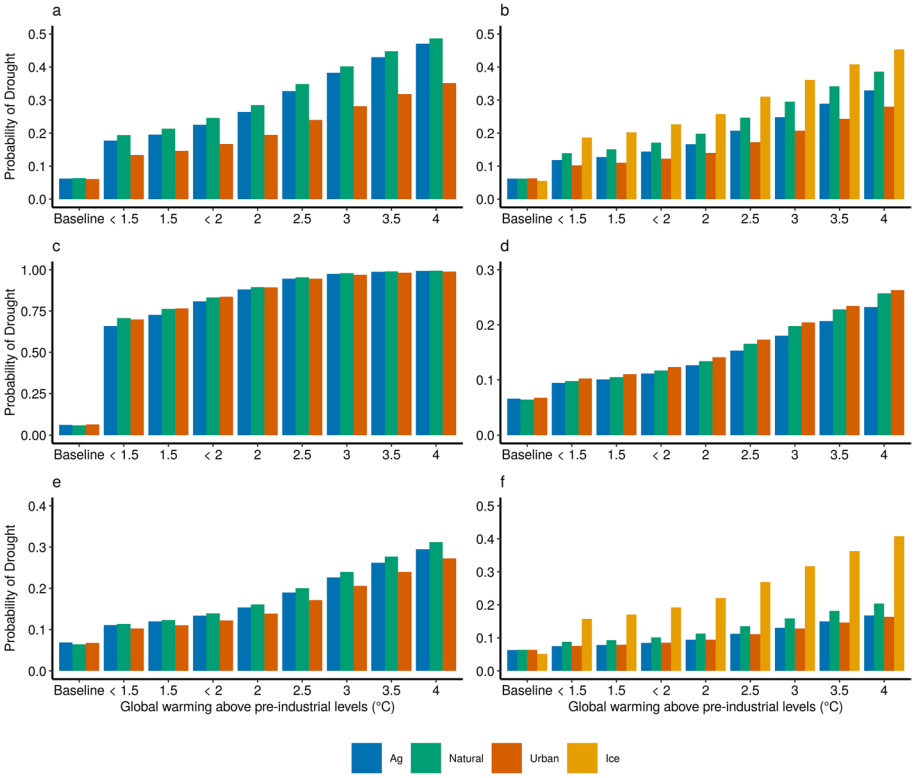

Fig. 1 Average monthly probability of an SPEI-12 meteorological drought of magnitude -1.5 in broad habitat categories (from ESA CCI, 2015) in **a**) Brazil **b**) China **c**) Egypt **d**) Ethiopia **e**) Ghana **f**) India. See SM Tables 1–6 for information broken down by finer land cover classification. Median based on 23 GCM patterns

The maximum number of consecutive months of severe drought in any given thirty-year period averaged over the entire country can be found in Table 3 and Fig. 2. This is an indication of the potential level of exposure and risk for systems that are impacted by long duration dry spells, such as the agricultural sector or human settlements largely dependent on rainfall. Table 4 and Fig. 3 shows the corresponding numbers of people exposed to drought.

Any amount of warming is projected to substantially increase the number of consecutive months of severe drought. Thus, in Brazil, China, Ethiopia, and Ghana droughts of

Table 3 Maximum number of consecutive months of a SPEI-12 < -1.5 intensity drought (classed as "severe") per each 30-year period at each grid cell, averaged over all grid cells in each of the six countries in the study. Median of results from 23 GCM patterns

Country	Baseline	< 1.5	1.5 °C	< 2	2.0 °C	2.5 °C	3.0 °C	3.5 °C	4.0 °C
Brazil	10.2	20.4	22.2	26.0	21.0	41.1	52.0	63.3	74.7
China	9.5	14.8	15.8	18.1	21.8	30.5	40.9	51.8	62.6
Egypt	9.5	87.0	108.3	150.0	197.3	265.4	309.1	330.4	339.0
Ethiopia	10.2	12.6	13.1	14.1	15.3	18.9	22.7	26.9	31.5
Ghana	12.0	15.4	16.0	16.9	18.3	20.9	24.8	29.2	33.8
India	10.9	11.2	11.4	11.7	12.3	13.6	15.3	17.3	19.3

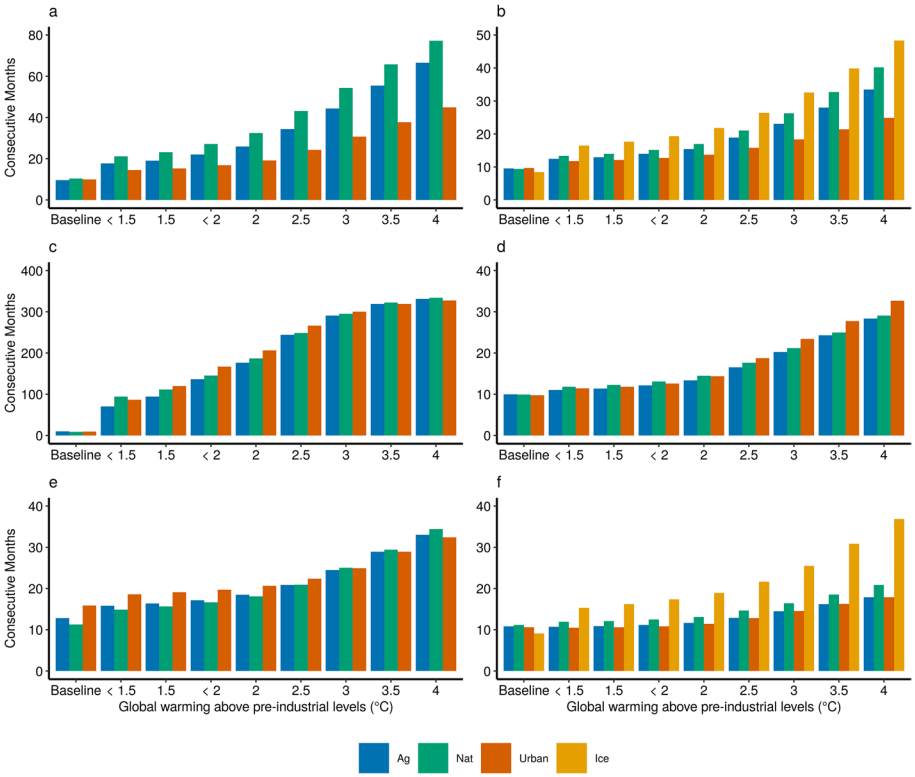

Fig. 2 Average maximum consecutive months of an SPEI-12 drought of magnitude -1.5 by broad habitat categories in **a**) Brazil **b**) China **c**) Egypt **d**) Ethiopia **e**) Ghana **f**) India. See SM Tables 7–12 for information broken down by finer land cover classification. Median based on 23 GCM patterns

longer than two years are projected to occur even in a 1.5 °C warming scenario. India nears this mark and in Egypt severe drought begins to become the new norm. In a 2 °C warming scenario, the length of droughts projected in all countries except India exceed three years. In a 3 °C warming scenario, droughts are projected to approach 4–5 years in length and in a 4 °C warming scenario, severe droughts of longer than five years are projected for Brazil and China, with severe drought the new baseline condition (sometimes referred to

Table 4 Additional people projected to be exposed to drought in 2100 due to climate change and socioeconomic change (compared to 1961–1990) expressed as a percentage of the population in 2100 (SSP2). Based on the median of the results from 23 GCMs

Country	< 1.5	1.5 °C	< 2	2.0 °C	2.5 °C	3.0 °C	3.5 °C	4.0 °C
Brazil	7.4	8.6	10.6	13.2	17.6	21.7	25.4	28.7
China	0.6	1.4	2.7	4.4	7.8	11.3	14.9	18.5
Egypt	67	73.9	81.4	87.4	92.5	94.6	95.6	96
Ethiopia	7.3	7.9	9.0	10.4	13.1	15.8	18.5	21
Ghana	8.0	9.5	10.1	12.1	15.5	19.5	23.0	26.2
India	3.2	3.6	4.1	5.0	6.6	8.3	10.1	11.8

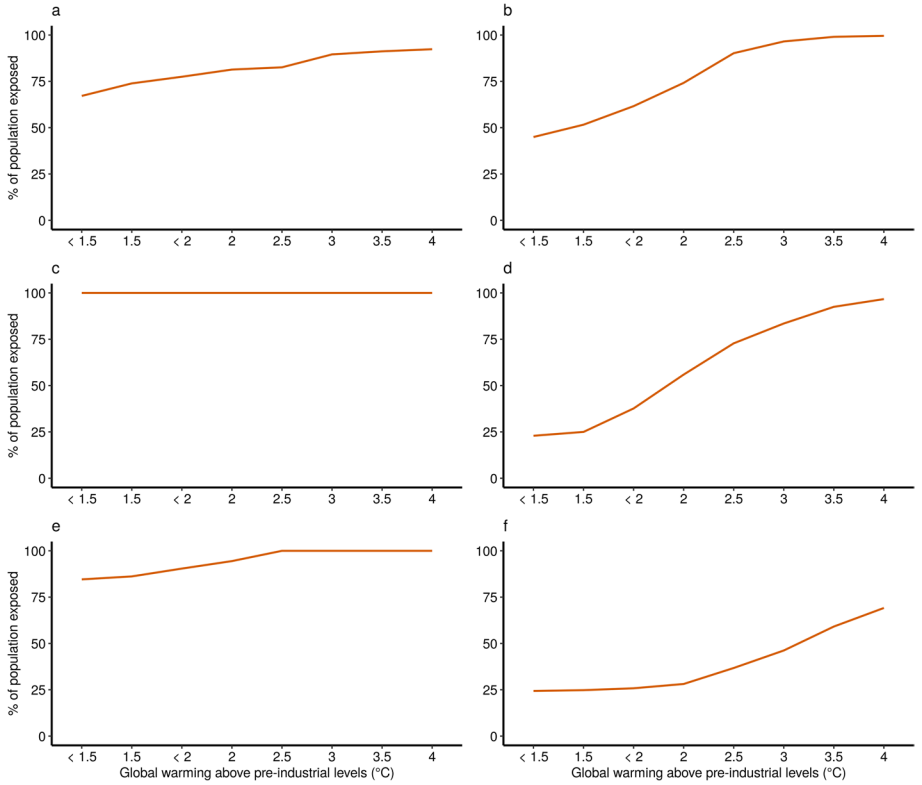

Fig. 3 Percent of population in 2100 (SSP2) projected to be exposed to a drought of at least 12 consecutive months in a 30-year period (SPEI-12, -1.5) in **a**) Brazil **b**) China **c**) Egypt **d**) Ethiopia **e**) Ghana **f**) India. Median based on 23 GCM patterns

as 'normal' condition) in Egypt. As with the probability calculations shown in Fig. 1, the increase in consecutive months of drought per 30-year period shown in Fig. 2 increases largely linearly with temperature. Significantly, it is worth noting that these values are averaged over the entire country. Thus, large countries containing many climatic zones would be expected to have lower overall averages, and zones with the strongest drying trends within the country may have much longer droughts than indicated by country-level average (Tables 2 and 3).

One way of dealing with the differences in geographic size is to examine drought by different geographic units. Fig. 1 shows the average monthly probability of severe drought by broad land cover categories. These categories include agriculture (agriculture greater than 50% of a 300 m pixel), natural land (greater than 50% natural), urban and areas of permanent snow and ice. A more refined breakdown of drought probability in individual land cover classes can be found in Supplemental Material Tables SM1-6.

In Brazil, there are large differences in drought probability between natural and agricultural areas (with high probabilities) and urban areas. This represents the history of areas where settlement was more likely to occur in places with less variable climate. In higher warming scenarios, this difference in probability of drought approaches 20%. Natural and agricultural areas have similar drought probabilities projected for all temperatures with

natural areas having slightly higher probabilities. In a 2 °C warming scenario, the drought probability projections in natural and agricultural areas approaches 30%, a value not reached in urban areas until the 3.5 °C warming scenario. In the 4 °C warming scenario, the drought probability projected in agricultural and natural areas approaches 50%. The increase in projected drought probabilities is generally linear with temperature (Fig. 1).

China shows similar patterns, with urban areas projected to have reduced probabilities of drought relative to natural and agricultural areas. Unlike Brazil, however, natural areas have a higher probability of drought than agricultural areas. One potential consequence of this is that, with increasing warming, shifting agriculture into areas currently identified as natural comes with a higher risk of potential drought.

Overall, the situation projected for Egypt is similar. As might be expected for an arid region, SPEI shows a rapid increase in projected probabilities of drought across all land cover types. Agricultural areas are projected to have slightly lower probabilities of drought until approximately the 2 °C warming scenario. Unlike Brazil and China, urban areas are projected to have a greater exposure to drought than agricultural areas. Drought probabilities are projected to be greater than 90% under the 2 °C warming scenario.

Similar to Egypt, urban areas in Ethiopia are projected to have a slightly higher drought probability than natural and agricultural areas, and agricultural areas a slightly lower probability than natural. Overall, however, drought probabilities in Ethiopia across the three land cover types are projected to remain low even with higher degrees of warming.

For agricultural, natural and urban areas, Ghana and India are projected to show similar patterns to Ethiopia. In Ghana, urban and agricultural areas are projected to have slightly lower probabilities of drought than natural areas, with urban areas having the lowest probabilities. As with China, this suggests that it might be difficult for agriculture to be shifted into natural areas without increased drought risk. Like China, India also shows a substantially higher probability of severe drought projected for areas with permanent snow and ice. This could potentially have the same negative impacts on long-term water storage in the Himalayas.

The overall patterns for the maximum consecutive months of severe drought (Fig. 2) are similar to those described above for Fig. 1. The models project that severe drought could potentially become the new norm for Egypt across all land cover types. Taking into account the time lag for SPEI-12, the maximum duration of drought in areas of permanent snow and ice is approximately three years in the 2 °C warming scenario in both China and India. In the 4 °C warming scenario, in China, nearly five-year duration droughts and four-your duration droughts in India are projected. Greater detail of the maximum consecutive months of severe drought in specific land cover types can be found in SM Tables 7–12.

The overall percentage of population in each country in 2100 (SSP2) exposed to severe drought, is shown in Fig. 3. These figures are for severe droughts lasting 12 months or longer in a 30-year period. In all cases, almost the entire population in each of the countries studied is projected to be exposed to severe droughts of this length, in a 30-year period, by the 4 °C warming scenario. Brazil and Egypt show rapid increases in the percentage population projected to be exposed to severe drought even in the 1.5 °C warming scenario. The population projected to be exposed in China increases steadily between the 1.5° and 2.5 °C warming scenarios, before it begins to plateau at greater than 90%. The percentage of population projected to be exposed in Ethiopia begins to increase in the 1.5 °C warming scenario and increases steadily to near 100% in the 4 °C warming scenario. In Ghana, the population projected to be exposed to severe drought of longer than one year is 100% by the 2.5 °C warming scenario. In India, the population projected to be exposed to severe drought does not significantly start to increase until after the temperatures reached in the 2 °C warming scenario. Note that even where the results in Fig. 3 plateau, they should not

be interpreted as indicating that the impacts do not become worse for higher warming levels. Instead they are likely to continue to worsen (e.g. Table 2), but in ways not captured by this metric.

The percentage of land in each of the broad land cover categories of Fig. 2 projected to be exposed to a severe drought of longer than 12 months in a 30-year period is given in Fig. 4. Overall, the percentage is projected to increase rapidly by the 1.5 °C warming scenario in Brazil, China and Egypt, and in areas of permanent snow and ice in India. Not only does the area exposed to drought increase with global warming, but it also increases non-linearly: there is clearly an inflection point above which the rate of increase of area accelerates markedly. This is projected to be the 2 °C warming scenario in Ethiopia, Ghana and for other habitat types in India. In Brazil and China, the percent of urban areas projected to be exposed to drought is substantially lower than other land cover types. Nevertheless, in the 1.5 °C warming scenario, greater than 50% of agricultural areas are projected to be exposed to severe droughts of a year or longer in Brazil, China, and Egypt. This is projected to occur at approximately the 2 °C warming scenario in Ethiopia, and closer to 3 °C in Ghana and India. In China, the potential projected impacts of drought on areas with permanent snow and ice is significant. These areas form the headwaters of many major river systems, and thus the water for millions of people downstream. Increasing probability and duration (Fig. 4b) of severe drought projects potential declines in water storage in the Chinese Himalayas in the form of snow and ice.

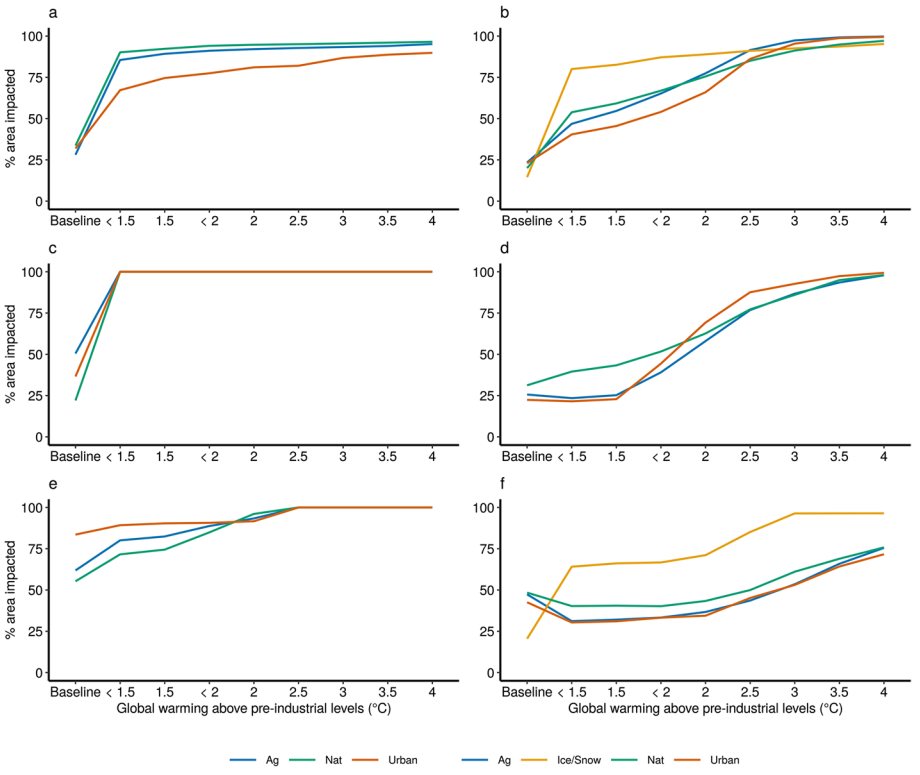

Fig. 4 Percent of area of a given land cover type projected to experience an SPEI-12 drought of greater than 12 months in any 30-year period in **a**) Brazil **b**) China **c**) Egypt **d**) Ethiopia **e**) Ghana **f**) India. Median of results from 23 GCMs

4 Discussion and conclusions

Drought, as indicated by SPEI12, is projected to increase greatly in all six countries studied as global temperatures rise, with large increases in the projected numbers of people and areal extent of agricultural land exposed to drought. For example, in the 3 °C warming scenario, more than 80% of the agricultural area in Brazil, China, Egypt and Ethiopia in any 30-year period are projected to be exposed to droughts of longer than one year. For Egypt and Ethiopia the corresponding figure is more than 50% in any 30-year period.

The SSP2 population scenario used here, describes a 'middle-of-the-road' development for all key drivers, including population, macro-economic and technology assumptions. In particular, the global population increases from 7.2 billion in 2015 to 9.2 billion by 2100 and global GDP from 81.1 trillion US$2005 in 2015 to 537 trillion by 2100.

Since the SSP2 is a middle of the road population projection, should population increases be larger, as in SSP reaching 12 billion by 2100, population exposure to drought might be underestimated. However, if populations are lower, 6 billion in 2100 and declining as in SSP1 they could be overestimated. It should be noted that the SSP2 scenario is considered consistent with a wide range of year 2100 radiative forcing levels from 1.9 to 7 W/m2 when combined with various climate change mitigation scenarios (O'Neill et al. 2020) accordingly resulting in global warming levels in 2100 from approximately 1.5 to 4 °C.

Meeting the long-term temperature goal of the Paris Agreement could benefit all of the countries in this study with Egypt potentially benefiting the most. However, the current pledges with the potential of reaching warming levels of 3 °C or more could impact all of the countries in this study. This indicates that all six of the countries will need to deal with water stress in the agricultural sector—potentially through shifting crop varieties or through irrigation, if water is available. The amount of adaptation required increases rapidly with global warming.

These findings are consistent with IPCC (Seneviratne et al. 2021) which projects increases in the exposure of terrestrial land to hydrological and ecological drought in N, SE and SW Africa, W Central and S Asia, and NE South America. IPCC (Seneviratne et al. 2021) global projections also include projections of increased drought in the Mediterranean, Australasia and Western N America, while there are smaller projections of increases in meteorological drought. While global precipitation levels also increase with warming, regionally there are marked contrasts in the projected trends, and when combined with the projected increase in the amount of precipitation falling in heavy precipitation events (Seneviratne et al. 2021), simultaneous increases in both floods and droughts may occur.

The increases in drought projected in this study show only partial agreement with the mean aridification identified by Park et al. (2018). The latter study found that aridification (that is, increases in aridity with a signal to noise ratio lower than -0.5) emerged from natural variability by 1.5C of warming in parts of Brazil and southern China, and by 2 °C in parts of Ghana and coastal Egypt, but no aridification in Ethiopia or India. This difference may be because Park et al. (2018) considered mean aridity (defined as the ratio of P to PET rather than the P minus PET difference used here in SPEI) and did not use a metric standardised against observed variability, in contrast to this study.

India and China both have large areas currently under 'permanent' ice and snow cover. However, in the 3 °C warming scenario, 90% of these areas are projected to face severe droughts lasting longer than a year in a 30-year period. Other natural areas are projected to be similarly impacted. Brazil, China, Egypt and Ethiopia are all projected to have 80%-100% of land classified as natural as being under severe droughts lasting longer than one

year; 60%-80% in Ghana and India. Adaptation options are largely impractical in the natural land sector, and while water supplies may be able to be created/maintained, increased fire risk, disease risk and mortality could all increase.

Urban areas fare only slightly better and generally show the same pattern as above. Areas along rivers/streams or with reservoirs may fare better (see water stress metrics, He et al 2022) depending on competition for water resources and headwater sources (e.g. Egypt, as the Nile originates in tropical countries less impacted by drought). However, urban areas more dependent on seasonal water replenishment could be harder hit. While this is true for small settlements dependent on replenishment of local water storage tanks and reservoirs, it can extend to larger cities (e.g. Las Vegas, Los Angeles, San Francisco and other western US cities dependent on reservoirs for water storage).

Thus, meeting the Paris Accords could have major benefits in terms of reducing severe drought risk in these six countries, in all major land cover classes and for large percentages of the population.

Supplementary Information The online version contains supplementary material available at https://doi.org/10.1007/s10584-022-03359-2.

Author contributions DVV provided the IMAGE scenarios, TO and CW created the pattern scaled climate projections, NF calculated SPEI parameters, RJ conducted literature review, and RW designed and led the work. JP performed the country level analyses, drew the figures and wrote the paper, to which all authors contributed.

Funding The research leading to these results received funding from the UK Department for Business, Energy & Industrial Strategy (BEIS). TJO also received support from the Belmont Forum and JPI-Climate project INTEGRATE funded by the Natural Environment Research Council (grant no. NE/P006809/1). We thank the members of BEIS Climate Science—International who provided feedback to the study and the manuscript.

Declarations

Conflict of interest The authors declare no competing interests.

Open Access This article is licensed under a Creative Commons Attribution 4.0 International License, which permits use, sharing, adaptation, distribution and reproduction in any medium or format, as long as you give appropriate credit to the original author(s) and the source, provide a link to the Creative Commons licence, and indicate if changes were made. The images or other third party material in this article are included in the article's Creative Commons licence, unless indicated otherwise in a credit line to the material. If material is not included in the article's Creative Commons licence and your intended use is not permitted by statutory regulation or exceeds the permitted use, you will need to obtain permission directly from the copyright holder. To view a copy of this licence, visit http://creativecommons.org/licenses/by/4.0/.

References

Aadhar S, Mishra V (2018) Impact of climate change on drought frequency over India. In Government of India. Climate Change and Water Resources in India. Ministry of Environment, Forest and Climate Change. (MoEF&CC), pp.117–129

Antwi-Agyei P, Fraser ED, Dougill AJ, Stringer LC, Simelton E (2012) Mapping the vulnerability of crop production to drought in Ghana using rainfall, yield and socioeconomic data. Appl Geogr 32(2):324–334. https://doi.org/10.1016/j.apgeog.2011.06.010

Du J, Fang J, Xu W et al (2013) Analysis of dry/wet conditions using the standardized precipitation index and its potential usefulness for drought/flood monitoring in Hunan Province, China. Stoch Environ Res Risk Assess 27:377–387. https://doi.org/10.1007/s00477-012-0589-6

Elkollaly M, Khadr M, Zeidan B (2018) Drought analysis in the Eastern Nile basin using the standardized precipitation index. Environ Sci Pollut Res 25:30772–30786. https://doi.org/10.1007/s11356-016-8347-9

Feyen L, Dankers R (2009) Impact of global warming on streamflow drought in Europe. J Geophys Res 114:D17116. https://doi.org/10.1029/2008JD011438

Gupta V, Jain MK (2018) Investigation of multi-model spatiotemporal mesoscale drought projections over India under climate change scenario. J Hydrology 567:489–509

Harris I, Jones PD, Osborn TJ, Lister DH (2014) Updated high-resolution grids of monthly climatic observations - the CRU TS3.10 Dataset. Int J Climatol 34:623–642. 10/f5tqvx

He Y, Manful D, Warren R et al (2022) Quantification of impacts between 1.5 and 4 °C of global warming on flooding risks in six countries. Clim Change 170:15. https://doi.org/10.1007/s10584-021-03289-5

James R, Washington R, Schleussner C-F, Rogelj J, Conway D (2017) Characterizing Half-a-degree Difference: A Review of Methods for Identifying Regional Climate Responses to Global Warming Targets. Wiley Interdiscip. Rev Clim Change 8:e457. 10/gdxrjz

Jones B, O'Neill BC (2016) Spatially explicit global population scenarios consistent with the Shared Socioeconomic Pathways. Environ Res Lett 11:084003

Leng G, Tang Q, Rayburg S (2015) Climate change impacts on meteorological, agricultural and hydrological droughts in China. Glob Planet Chang 126:23–34

Marengo JA, Torres RR, Alves LM (2017) Drought in Northeast Brazil—past, present, and future. Theor Appl Climatol 129:1189–1200. https://doi.org/10.1007/s00704-016-1840-8

Naresh Kumar M, Murthy CS, SeshaSai MVR, Roy PS (2011) Spatiotemporal analysis of meteorological drought variability in the Indian region using standardized precipitation index. Met Apps 19:256–264. https://doi.org/10.1002/met.277

Oguntunde PG, Abiodun BJ, Lischeid G (2017) Impacts of climate change on hydro-meteorological drought over the Volta Basin, West Africa. Glob Planet Chang 155:121–132. https://doi.org/10.1016/j.gloplacha.2017.07.003

Osborn TJ, Wallace CJ, Lowe JA, Bernie D (2018) Performance of pattern-scaled climate projections under high-end warming, part I: surface air temperature over land. J Clim 31:5667–5680. https://doi.org/10.1175/JCLI-D-17-0780.1

Osborn TJ, Wallace CJ, Harris IC, Melvin TM (2016) Pattern scaling using ClimGen: monthly-resolution future climate scenarios including changes in the variability of precipitation. Clim Chang 134:353–369. 10/f795rk

Park C, Jeong S, Joshi M et al (2018) Keeping global warming within 1.5 °C constrains emergence of aridification. Nat Clim Chang 8:70–74. https://doi.org/10.1038/s41558-017-0034-4

Pathak AA, Dodamani BM (2019) Comparison of Meteorological Drought Indices for Different Climatic Regions of an Indian River Basin. Asia-Pacific J Atmos Sci. https://doi.org/10.1007/s13143-019-00162-5

Penalba OC, Rivera JA (2015) Regional aspects of future precipitation and meteorological drought characteristics over Southern South America projected by a CMIP5 multi-model ensemble. Int J Climatol 36:974–986. https://doi.org/10.1002/joc.4398

Qin Z, Tang H, Li W, Zhang H, Zhao S, Wang Q (2014) Modelling impact of agro-drought on grain production in China. Int J Disaster Risk Reduct 7:109–121. https://doi.org/10.1016/j.ijdrr.2013.09.002

Seneviratne SI, Zhang X, Adnan M, Badi W, Dereczynski C, Di Luca A, Ghosh S, Iskandar I, Kossin J, Lewis S, Otto F, Pinto I, Satoh M, Vicente-Serrano SM, Wehner M, Zhou B (2021) Weather and Climate Extreme Events in a Changing Climate. In: Climate Change 2021: The Physical Science Basis. Contribution of Working Group I to the Sixth Assessment Report of the Intergovernmental Panel on Climate Change. In: Masson-Delmotte V, Zhai P, Pirani A, Connors SL, Péan C, Berger S, Caud N, Chen Y, Goldfarb L, Gomis MI, Huang M, Leitzell K, Lonnoy E, Matthews JBR, Maycock TK, Waterfield T, Yelekçi O, Yu R, Zhou B (eds). Cambridge University Press

Stehfest E, van Vuuren D, Bouwman L, Tom Kram (2014) Integrated Assessment of Global Environmental Change with IMAGE 3.0: Model Description and Policy Applications. Netherlands Environmental Assessment Agency (PBL)

Tebaldi C, Arblaster JM (2014) Pattern scaling: Its strengths and limitations, and an update on the latest model simulations. Clim Change 122:459–471. 10/f5rp2w

Vicente-Serrano SM, Beguería S, López-Moreno JI (2010) A Multiscalar drought index sensitive to global warming: the standardized precipitation evapotranspiration index. J Clim 23:1696–1718. 10/c84fcq

Wang L, Chen W (2014) A CMIP5 multimodel projection of future temperature, precipitation, and climatological drought in China. Int J Climatol 34:2059–2078. https://doi.org/10.1002/joc.3822

Wang L, Chen W, Zhou W (2014) Assessment of future drought in Southwest China based on CMIP5 multimodel projections. Adv Atmos Sci 31(5):1035–1050. https://doi.org/10.1007/s00376-014-3223-3

Wang D, Jenkins K, Forstenhäusler N et al (2021) Economic impacts of climate-induced crop yield changes: evidence from agri-food industries in six countries. Clim Change 166:30. https://doi.org/10.1007/s10584-021-03062-8

Zhao MAG, Velicogna I, Kimball JS (2017) A Global Gridded Dataset of GRACE Drought Severity Index for 2002–14: Comparison with PDSI and SPEI and a Case Study of the Australia Millennium Drought. J Hydrometeorol 18(8):2117-2129

Publisher's note Springer Nature remains neutral with regard to jurisdictional claims in published maps and institutional affiliations.